Photoionization of the barium 4d subshell including relativistic and relaxation effects

Vojislav Radojević, Mickey Kutzner, and Hugh P. Kelly
Department of Physics, University of Virginia, Charlottesville, Virginia 22901
(Received 7 November 1988; revised manuscript received 27 March 1989)

Calculations of photoionization parameters are presented for the 4*d* shell of atomic Ba. A sequence of calculations was performed in the framework of the relativistic random-phase approximation: (i) including correlations within the 4*d* shell only; (ii) including correlations arising from coupling with 5*s*, 5*p*, and 6*s* shells; and (iii) including relaxation of the 4*d* shell. These results are compared with some other theoretical calculations and with recent experimental data.

I. INTRODUCTION

Recent measurements[1–4] of the 4*d* partial photoionization cross section of Ba have stimulated us to attempt to understand the photoionization of atomic barium in detail. Photoemission results by Becker *et al.*[1,2] and by Wuilleumier[3] for the 4*d* cross section appear to be considerably smaller than all existing theoretical results.[5–11] In earlier experimental works[12–14] the total photoabsorption cross section was measured in relative units, and by normalizing these data appropriately, good agreement with calculated results has been obtained. Hecht and Lindau performed photoelectron spectroscopy measurement[15] on Ba in the solid phase to obtain the 4*d* partial cross section. Very recent measurements by Richter *et al.*[4] have yielded the 4*d* plus satellite cross section for atomic barium. The measurements by Becker *et al.*[1,2] and by Wuilleumier[3] appeared to be the first measurement of the 4*d* main-line cross section performed on atomic barium.

Calculations have been performed using various approaches such as the Hartree-Slater method,[5] the Hartree-Fock method (HF),[6] many-body perturbation theory[6] (MBPT), and the random-phase approximation with exchange (RPAE).[6–9] There have been RPAE calculations including some of the diagrams describing relaxation.[7] Relaxation effects were accounted for by using relaxed orbitals in the RPAE (Ref. 9) and the HF (Ref. 10) calculations. There are also calculations performed in the time-dependent local density approximation (TDLDA).[11]

It has been shown that the relaxation of the atomic ion must be included[7,9,10] to bring the shapes of calculated cross sections into agreement with the shapes of experimental curves.[12–15] In all theoretical results in which relaxation effects are not explicitly included,[5,6,8] with the exception of the TDLDA calculation,[11] the cross section has a relatively high and narrow peak a few eV above the 4*d* threshold. The inclusion of relaxation effects in calculations[7,9,10] significantly lowered and flattened the peak in the cross section and moved it towards higher energies, bringing the shape of the cross section in closer agreement with the measured shape.

In order to understand the new experimental data,[1–3] we performed a sequence of relativistic calculations of the random-phase approximation (RPA) type, which we describe in this paper. The RPA method has been reviewed for the nonrelativistic case[16] (RPA with exchange –RPAE) and for the relativistic case (relativistic RPA—RRPA).[17] We note that when all channels are coupled both RPAE and RRPA are gauge invariant, i.e., the length and velocity results are identical to within numerical accuracy. First we performed calculations using channels arising from excitations of the 4*d* shell only, as was also done in previous nonrelativistic, RPAE calculations.[6–8] We then included coupling with channels coming from excitation of adjacent 5*s*, 5*p*, and 6*s* shells, and we finally included relaxation of the 4*d* shell. It was found that the results of photoionization calculations, especially for the cross sections, are sensitive to inclusion of various effects accounted for in the present work, and that inclusion of all these effects is essential to bring the theoretical results into agreement with the recent experimental data.[1–3]

The methods and types of calculations used in the present work are described in Sec. II. Section III is devoted to the presentation and discussion of our results, while Sec. IV contains concluding remarks.

II. METHODS AND CALCULATIONS

We performed initial calculations in the RRPA (Ref. 17) including only channels obtained by dipole excitations of the 4*d* subshells (truncated RRPA). There are six such *jj*-coupled channels:

$$4d_{3/2} \rightarrow f_{5/2},\ p_{3/2},\ p_{1/2}\ ,$$
$$4d_{5/2} \rightarrow f_{7/2},\ f_{5/2},\ p_{3/2}\ .$$

In these calculations only relativistic effects should be responsible for differences with respect to the previous nonrelativistic, RPAE results[6,8] which are discussed below. Then additional channels, obtained by dipole excitation of 5*s*, 5*p*, and 6*s* shells, were included in our RRPA calculations, making a total of 15 coupled channels. The additional channels are

$$5s_{1/2} \rightarrow p_{3/2},\ p_{1/2}\ ,$$
$$5p_{1/2} \rightarrow d_{3/2},\ s_{1/2}\ ,$$

 ©1989 The American Physical Society

$5p_{3/2} \rightarrow d_{5/2},\ d_{3/2},\ s_{1/2}$,

$6s_{1/2} \rightarrow p_{3/2},\ p_{1/2}$.

Finally, 15-channel RRPA-type calculations were performed taking into account relaxation of the $4d$ subshell (RRPA-R calculations). In these RRPA-R calculations the V^{N-1} potential in which an excited electron moves is calculated using relaxed orbitals obtained by a self-consistent calculation of the $N-1$ electron ion with the hole in the $4d_{5/2}$ subshell. Results were not significantly different at a few energy points when the relaxed orbitals were calculated with the hole in the $4d_{3/2}$ subshell.

The theoretical values of the $4d$ thresholds in strict RRPA calculations are the absolute values of the Dirac-Hartree-Fock (DHF) orbital eigenvalues. In the relaxed calculations the differences between the self-consistently calculated total energies of the corresponding ionic core and the neutral atom (ΔE_{SCF} values) are used for the $4d$ thresholds. In all calculations, the DHF eigenvalues are used for the values of other than $4d$ thresholds ($5s$, $5p$, and $6s$). All relevant calculated threshold energies are presented in Table I, where they are compared with the experimental values.[18] One can see that for all considered subshells except the outermost $6s$ one, the ΔE_{SCF} values agree better with the experimental data than the DHF values. The ΔE_{SCF} values for the $4d$ thresholds agree with the experimental values to within 0.6%. It is anticipated that by performing multiconfiguration calculations (which are beyond the scope of the present study) the $6s$ ΔE_{SCF} threshold value would also agree better with the measured value than the DHF threshold does.

As is well known, the RPA, whether in its nonrelativistic version (RPAE) or in the relativistic form (RRPA), is a gauge-invariant theory, so that the results in all gauges coincide.[16] The two most commonly used gauges are the so-called length and velocity form. Since the RPA includes all possible particle-hole excitations of all atomic subshells leading to the inclusion of a relatively large number of channels for heavier atomic systems, one often neglects the excitations of subshells far from the considered one because they are weakly coupled. Such a truncated RPA method is not exactly gauge invariant, but if the neglected channels arise from distant subshells, one obtains results very close to the complete, nontruncated RPA. The results in different gauges often almost coincide, their relative difference never exceeding a few percent. However, the RRPA-R approach, used in the present work, is not a gauge-invariant method, and the complete coincidence of various gauges is not expected, but one does expect the reasonable closeness of the results in different gauges if important and significant correlations are taken into account. This is confirmed by our results presented in Sec. III. Although the RRPA-R is not a strict RPA approach, the calculational procedure is identical to the RRPA method, except that excited orbitals are calculated in the field of the relaxed ion and corrections are made for the nonorthogonality of orbitals in the initial and final states. In addition, the ΔE_{SCF} energies are used to replace single-particle energy eigenvalues for the ionization thresholds.

TABLE I. Photoionization thresholds in eV for subshells of Ba included in the present calculations. The calculated DHF values and ΔE_{SCF} values are compared with the experimental data taken from the review by H. Siegbahn and L. Karlsson (Ref. 18).

Subshell	DHF[a]	ΔE_{SCF}[b]	Expt.
$4d_{3/2}$	106.49	100.60	101.0
$4d_{5/2}$	103.75	97.95	98.5
$5s$	43.63	41.82	
$5p_{1/2}$	26.03	24.31	24.7
$5p_{3/2}$	23.75	22.14	22.8
$6s$	4.44	4.28	5.21

[a]Absolute value of single-particle eigenvalue from Dirac-Hartree-Fock (DHF) calculations.

[b]Difference of self-consistent DHF calculations for ground state and ionic state.

In performing the calculations with relaxed orbitals, care was taken to calculate properly overlaps between relaxed and unrelaxed orbitals of the final and initial states. The many-body zeroth-order dipole matrix elements—by which all photoionization parameters, such as cross sections, angular asymmetry, and spin-polarization parameters are expressed[17]— are of the form

$$\langle \Phi_n | \mathcal{D} | \Phi_0 \rangle = \gamma \langle \varphi'_\epsilon | D | \varphi_i \rangle ,$$

where Φ_0 is the ground-state configuration wave function constructed from the unrelaxed self-consistent orbitals, Φ_n is the excited-state wave function for the channel n constructed from the relaxed orbitals for $(N-1)$ core electrons and one excited (continuum or virtually excited) orbital φ'_ϵ calculated in the field of the $(N-1)$ electrons. The orbital φ_i is the unrelaxed orbital of the corresponding hole, and $\mathcal{D}=\sum_{k=1}^{N} D(k)$ and D are respective many-particle and one-particle dipole operators. The factor γ is the overlap of the $(N-1)$-particle core states, obtained from the ground-state configuration by setting the hole for a given channel, and constructed from unrelaxed and relaxed orbitals. The factor γ describes an average loss of input flux into other reaction channels not accounted explicitly, e.g., double electron excitations (photoionization with excitation). In the above expression for the dipole matrix elements, the overlaps of the excited orbitals $\varphi'_{\epsilon p}$ and the ground-state unrelaxed p orbitals φ_i are neglected, and the $\varphi'_{\epsilon f}$ orbitals are automatically orthogonal to all ground-state orbitals. The overlaps γ are calculated in our codes by evaluating a determinant of the relevant matrices of overlaps of unrelaxed and relaxed orbitals. In previous calculations with relaxed orbitals[8,9] the overlaps γ are assumed to be one, while our calculations gave values between 0.89 and 0.95, depending on the hole. Calculation of the factor γ has the important effect of reducing the partial $4d$ cross section by approximately 20%.

The calculations in the strict RRPA calculations were performed with the codes used previously to study the noble gases and other closed-shell atomic systems.[19,20] The ground-state orbitals for these calculations were calculated with the DHF code designed for the RRPA photoionization code.[17] The photoionization code was then modified for the RRPA-R calculations: (a) to work with both relaxed orbitals to calculate the V^{N-1} potential and unrelaxed ground-state orbitals; (b) to read in unrelaxed and relaxed orbitals computed with the Oxford multiconfiguration Dirac-Fock package by Grant *et al.*[21] (used in this work in the single-configuration mode and producing the same unrelaxed orbitals as the DHF code); and (c) the part of the code for calculation of the overlaps was written, and overlaps were incorporated in the evaluation of the dipole matrix elements.

III. RESULTS AND DISCUSSION

To demonstrate the evolution of the calculated $4d$ cross section when relativistic effects, intershell couplings, and relaxation effects are successively included, we present results of these different calculations in Fig. 1. The previous nonrelativistic RPA (RPAE) results by Amusia *et al.*,[9] shown in Fig. 1, were performed including only channels obtained by dipole excitations of the $4d$ shell (i.e., including only intrashell correlations), and therefore should be the nonrelativistic counterpart of our six-channel RRPA results. Only averages of length and velocity gauge of theoretical results are presented in Fig. 1. The relative difference between these two forms is small, never exceeding 8–9 % for our theoretical results. The length-velocity difference in the RRPA calculations is a result of truncation, i.e., neglect of certain channels. As expected, these two forms are closest for the RRPA($4d+5s+5p+6s$) results (2–4 %), somewhat more different for the RRPA($4d$) results (3–5 %), and most different for the RRPA-R results (5–9 %). Usually, relative differences between these two gauges are larger at higher energies, where cross sections are smaller, but the absolute differences are then smaller. The length and velocity gauge RRPA-R results may not coincide, since such an approximation is not gauge invariant. However, the relative difference is still rather small (less than 9%). The shift of the low-energy start of the RPAE and RRPA cross-section curves in Fig. 1 is due to the difference between Hartree-Fock (nonrelativistic) and DHF (relativistic) values for the $4d$ thresholds. We were not able to perform RRPA-R calculations in the vicinity of the $4d_{3/2}$ threshold (until 1.5 eV above the threshold) because of instability experienced with our computer codes. We also did not perform any of our calculations between the $4d_{5/2}$ (lower) and $4d_{3/2}$ (higher) threshold, since this region is dominated by autoionizing resonances.

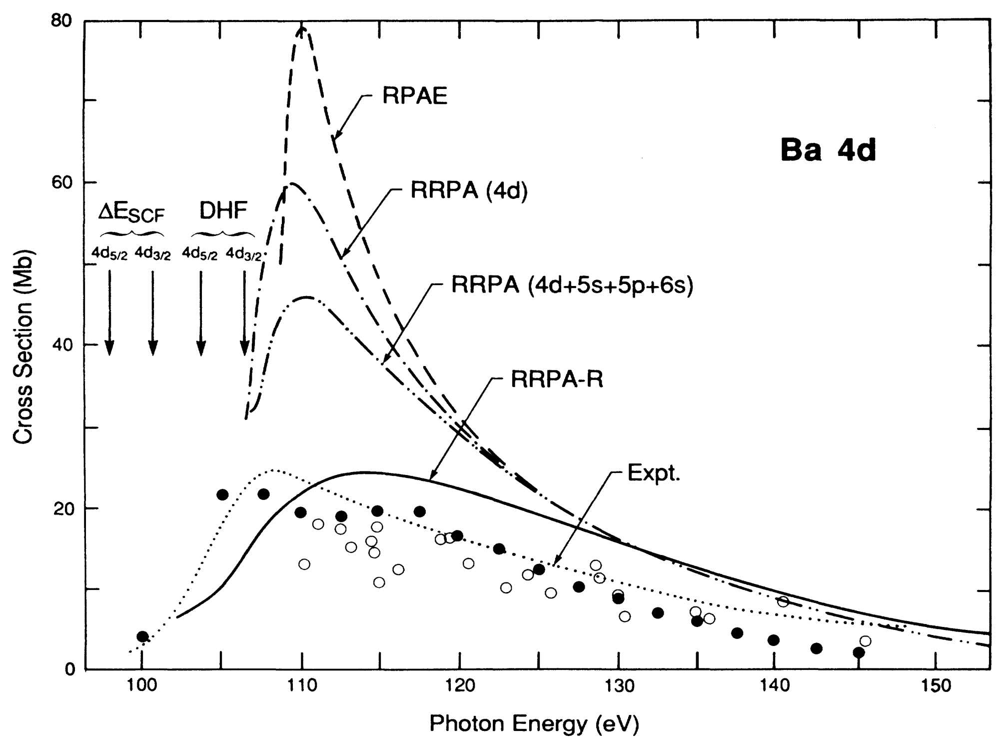

FIG. 1. Photoionization cross section for the $4d$ shell of Ba—the evolution of the cross section when relativistic effects, intershell couplings, and relaxation effects are included. RPAE: Nonrelativistic RPAE calculations by Amusia *et al.* (Ref. 9); RRPA($4d$): relativistic RRPA calculations with only $4d$ intrashell correlations included (six-channel calculation), present work; RRPA($4d+5s+5d+6s$): relativistic RRPA calculations with intershell correlations included (15-channel calculation), present work; RRPA-R: relativistic RRPA-like calculations using relaxed orbitals and with intershell correlations included (15 channels), present work; Expt.: experimental data from Ref. 1; ●, experimental data from Ref. 2; ○, experimental data from Ref. 3. (The error bars for the experimental data from Refs. 2 and 3 are not shown; one can see the error bars in Fig. 2 where the same experimental data are shown on larger scale.) Only averages of length and velocity gauge theoretical results are presented. The relative difference of all our results in length and velocity gauge does not exceed 9%.

One sees from Fig. 1 that relativistic effects lower the peak of the 4*d* cross-section curve from about 79 to 60 Mb. The inclusion of the intershell correlations (i.e., inclusion of channels originated by exciting other than 4*d* shells) in our RRPA calculations (15-channel calculation) lowers the peak even more to about 46 Mb. However, the peak is still much higher than the peak (25 Mb) in the recent experimental data,[1-3] also presented in Fig. 1. The inclusion of relaxation effects in our 15-channel RRPA-R calculations, using relaxed orbitals to calculate the V^{N-1} potential in which the excited or ionized electron moves, brings the peak of the calculated cross section, shown also in Fig. 1, into agreement with the height of the experimental peak. We wish to point out that the total experimental cross section[1-3] from which the partial 4*d* cross section was extracted is normalized to the results of the TDLDA calculations by Zangwill and Soven.[11]

The present RRPA-R results for the 4*d* cross section, including relaxation of the 4*d* shell, are again shown in Fig. 2, and compared there with two other calculations, which include relaxation effects in a way similar to the present work, and with the experimental data.[1-2] These two other calculations, both nonrelativistic and both using relaxed orbitals to calculate the V^{N-1} potential, are the RPAE-R results by Amusia *et al.*[9] and very recent MBPT results by Kutzner *et al.*[22] The RPAE-R results[9] include only channels with dipole excitations of the 4*d* shell (i.e., including only correlations within the 4*d* shell), and the $(N-1)$-particle overlap γ in the dipole matrix element is assumed to be one. The MBPT calculations include six *LS*-coupled channels equivalent to the present 15-channel calculations (the channels arising from excitation of 4*d*, 5*s*, 5*p*, and 6*s* shells) taking into account essentially the same important diagrams included in the RPA. The $(N-1)$-particle overlap γ is included in these calculations. The MBPT calculations were performed using the theoretical Hartree-Fock values of thresholds, and afterwards the calculated cross-section curves were shifted from the HF to the mean experimental 4*d* threshold. One can consider this MBPT result as the nonrelativistic counterpart of the present relativistic calculation including relaxation effects.

The three theoretical results presented in Fig. 2 show an evolution of the calculations with relaxation when intershell correlations and then relativistic effects are included. Inclusion of these effects has a similar effect on the cross section with relaxation as on the unrelaxed results shown in Fig. 1. Thus one sees that inclusion of other channels besides those obtained by exciting the 4*d* shell lowers the cross-section peak from about 43 to about 28 Mb; additional inclusion of relativistic effects

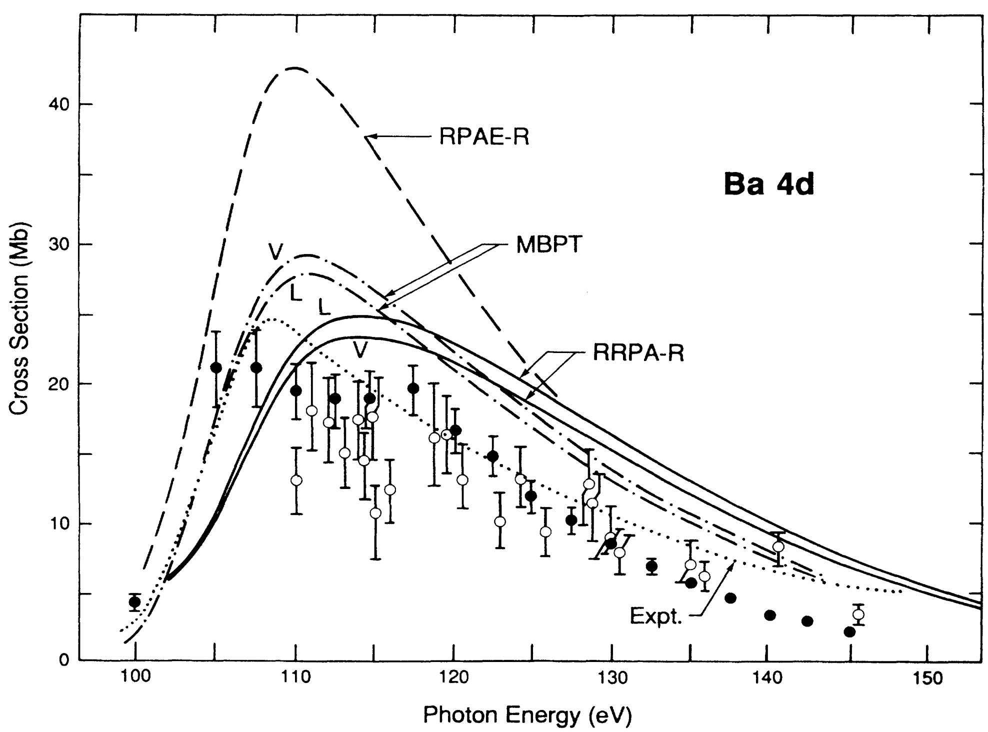

FIG. 2. Photoionization cross section for the 4*d* shell of Ba—comparison of the presently calculated relaxed cross section with some other relaxed calculations, and with the experimental data. RRPA-R: relativistic RRPA-like calculations using relaxed orbitals and with intershell correlations included (15 channels) in length (*L*) and velocity (*V*) gauge, present work; RPAE-R: nonrelativistic RPAE calculations using relaxed orbitals (Ref. 9); MBPT: nonrelativistic MBPT calculations by Kutzner *et al.* (Ref. 22) in length (*L*) and velocity (*V*) gauge; Expt.: experimental data from Ref. 1; ●, experimental data from Ref. 2; ○, experimental data from Ref. 3.

brings the peak into agreement with the height of the experimental peak, as already seen above. According to Fig. 2, it would appear that the MBPT results[22] agree better with the experimental data[1–3] than our RRPA-R results, except for the height of the peak of the cross section. However, the MBPT results were shifted in energy towards lower photon energies to bring the calculated threshold in agreement with the experimental one. If the MBPT results are shifted back so that the threshold coincides with the RRPA-R threshold, then both results are in reasonable agreement, except for the overall height. The lower peak in the RRPA-R result is a consequence of relativistic effects, as in the case of unrelaxed results (Fig. 1).

In Fig. 3 our calculated results for the $4d_{5/2}/4d_{3/2}$ branching ratio are compared with the experimental data.[2] The experimental and theoretical results agree reasonably at higher energies, although it is not possible to say whether our results with (RRPA-R) or without (RRPA) inclusion of relaxation effects agree better with the experimental data. However, measured and calculated results do not agree near the threshold.

The results of the relativistic RPA calculations for the photoelectron angular distribution asymmetry parameter of 4*d* shell are presented in Fig. 4 and compared there with other theoretical results[9,22] and with experimental data.[2] Only the average asymmetry parameter $\beta(4d)$ for the 4*d* shell is presented, which is expressed in terms of asymmetry parameters $\beta(4d_{3/2})$ and $\beta(4d_{5/2})$ of the respective $4d_{3/2}$ and $4d_{5/2}$ subshells as

$$\beta(4d)=\frac{\sigma(4d_{3/2})\beta(4d_{3/2})+\sigma(4d_{5/2})\beta(4d_{5/2})}{\sigma(4d_{3/2})+\sigma(4d_{5/2})},$$

where $\sigma(4d_{3/2})$ and $\sigma(4d_{5/2})$ are corresponding partial cross sections. The length and velocity gauge results for both strict RRPA and RRPA-R results practically coincide on the scale of Fig. 4. It is interesting to note that the strict RRPA results with interchannel correlations and without them (i.e., with only intrachannel correlations) also practically coincide in the figure. The recent MBPT results[22] are also plotted in Fig. 4. Although all these theoretical results are rather close one to another, they all are somewhat different from experimental data[2] presented also in Fig. 4.

We also calculated the spin-polarization parameters for the 4*d* shell. We are not aware of any other calculations nor measurements of these parameters for the 4*d* shell of barium. The spin polarization[23] is usually described by four dimensionless parameters ξ, η, ζ, and δ, which are expressed in terms of dipole matrix elements.[24,20] The parameters ξ, η, and ζ are directly related to the components of the spin-polarization vector, while the parameter $\delta=(\zeta-2\xi)/3$ is related to the spin polarization of the total photoelectron flux.[24,20] The results of our RRPA and RRPA-R calculations for all four parameters are presented in Fig. 5. One can see that the RRPA and RRPA-R results for spin parameters show the same trend

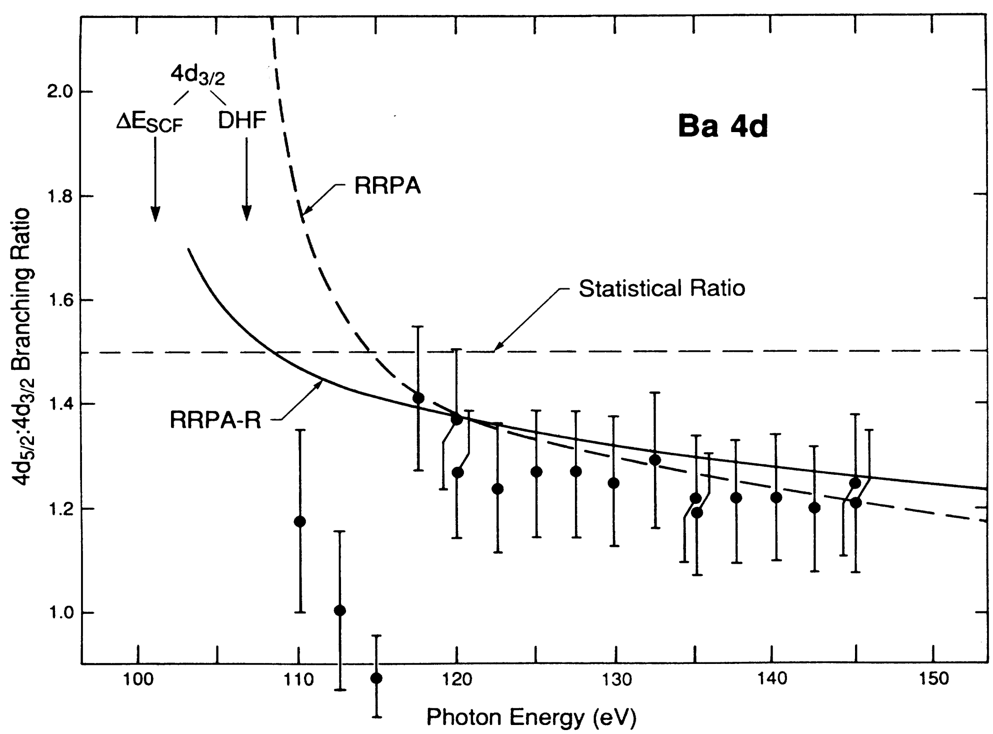

FIG. 3. $4d_{5/2}$:$4d_{3/2}$ branching ratio for Ba. RRPA: relativistic RRPA results, present work. There is no significant difference between the results including intershell correlations (15-channel calculation) and including only intrashell correlations (six-channel calculation). RRPA-R: relativistic RPA-like results calculated using relaxed orbitals and with intershell correlations included (15-channel calculation), present work. The length and velocity gauge calculation results coincide in the scale of the figure. Black circles (●) represent the experimental data (Ref. 2).

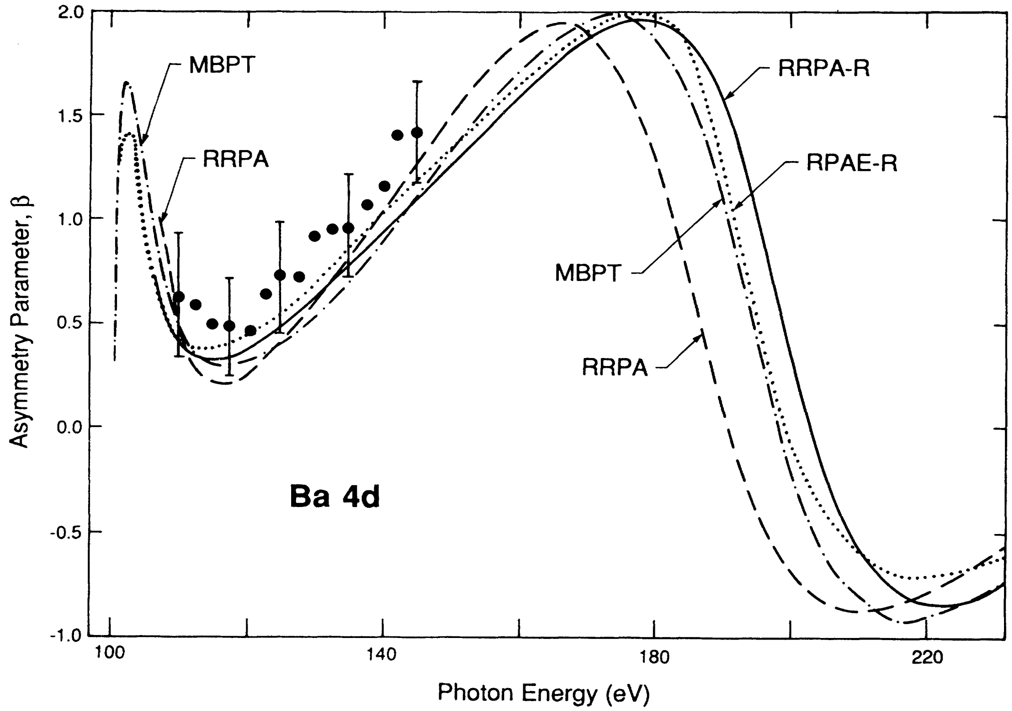

FIG. 4. Photoelectron angular distribution asymmetry parameter for the $4d$ shell of Ba. RRPA: relativistic RPA results, present work. There is no significant difference between the results including intershell correlations (15 channels) and including only intrashell correlations (six channels). RRPA-R: relativistic RPA-like results calculated using relaxed orbitals and with intershell correlations included (15 channels), present work; MBPT: nonrelativistic MBPT calculations by Kutzner *et al.* (Ref. 22); ●, experimental data (Ref. 2). The length and velocity gauge calculation results practically coincide in the figure.

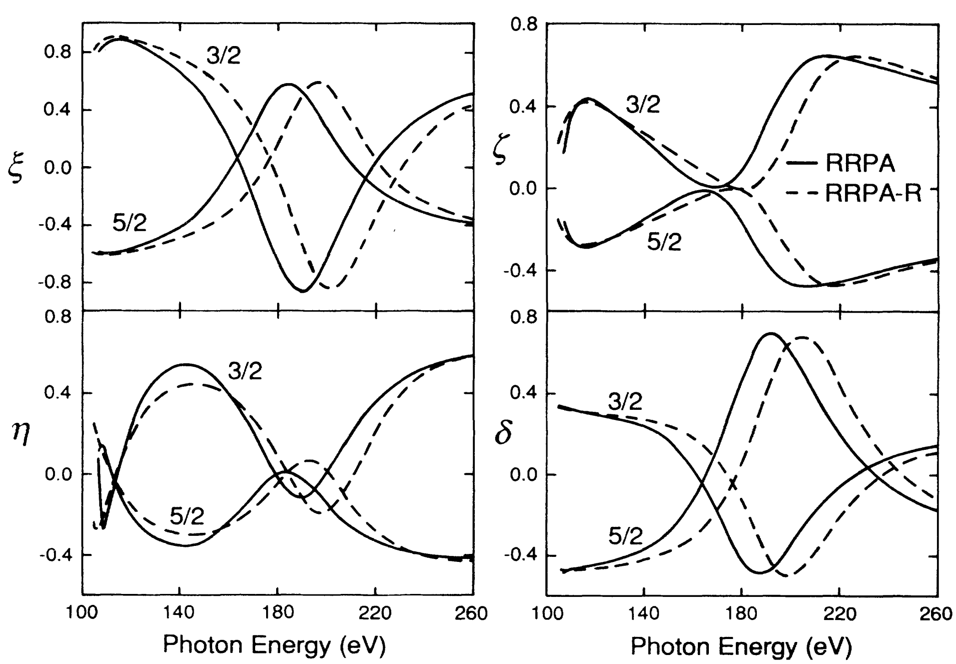

FIG. 5. Photoelectron spin-polarization parameters ξ, η, ζ, and δ for the $4d$ shell of Ba. Solid lines (——) represent the results of our RRPA calculations, while dashed lines (— — —) represent our RRPA-R results. The curves for the $4d_{3/2}$ and $4d_{5/2}$ subshells are labeled by their respective j values ($\frac{3}{2}$ and $\frac{5}{2}$). Length and velocity gauge results practically coincide in the figure.

in their energy dependence and do not differ as much for the spin-polarization parameters as for the cross section. The RRPA-R curves for polarization parameters look like the corresponding curves of the RRPA results shifted towards higher photon energies.

IV. CONCLUDING REMARKS

By including additional interchannel correlations, relativistic effects, and overlap integrals between the relaxed and unrelaxed orbitals, we have obtained smaller values for the 4*d* cross section of Ba than previous calculations[5–11] and better agreement with the recent experimental data.[1–3] In spite of the reasonably good agreement of our results including relaxation and relativistic effects with the experimental data,[1–3] there are still some discrepancies, since the experimental data are lower than our results at higher energies. These discrepancies may be due in part to the absence of double electron excitations in our calculations. Another possible reason for the discrepancies is that the approach with the V^{N-1} potential calculated using relaxed orbitals is equivalent to the assumption that the atomic ionic core is fully relaxed during the photoionization process, although relaxation is in general less than complete, especially at higher energies. Relaxation effects are much stronger for barium than for the noble gases, but it is possible that the degree of relaxation for barium is not as complete as described by the present relaxed calculations.

The theoretical cross-section results for the 4*d* shell of barium are considerably more sensitive to the inclusion of various effects than the corresponding results for xenon, which differs from barium only by the absence of the $6s^2$ shell. We believe that this is due to the well-known effective double-well structure of the potential for an *f* electron excited from the 4*d* shell.[25] For atoms in the vicinity of $Z=56$ (barium) the *f* electron is on the verge of changing (with increasing *Z*) from being primarily in the outer well to being primarily in the inner well.[25,26] With the increase of energy the *f* electron, which is mostly bound in the outer well at lower energies, penetrates the potential barrier more and eventually contracts (collapses) into the inner well, producing known resonance-like structure on the 4*d* cross section.[27] Small changes of the potential may significantly alter the presence of the *f* electron in one or another potential well and change also significantly the shape of the cross section. The barium atom seems to be particularly sensitive to the changes of potential due to inclusion of various effects. The other reason for differences of photoionization process between xenon and barium is the presence of the 6*s* electrons in the ground-state configuration of Ba, which are bound more loosely than other electrons and therefore are more sensitive to any change of atomic structure, e.g., to the presence of a hole in the 4*d* shell. For example, the 6*s* electron can be excited easily and therefore we expect greater contribution of the photoionization with excitation, which was approximately taken into account in the present work by overlaps between relaxed and unrelaxed orbitals.

ACKNOWLEDGMENTS

The authors are grateful to Dr. U. Becker and Dr. H. Kerkhoff for making their results available[2] in advance of publication, and also to Dr. F. Wuilleumier for providing his unpublished data.[3] The authors would like to thank Professor W. R. Johnson for use of his DHF and photoionization RRPA codes in this work. We also wish to thank Dr. J. W. Cooper for very helpful discussions. This work was supported in part by the National Science Foundation. A computational grant from the Academic Computing Center of the University of Virginia is gratefully acknowledged.

[1]U. Becker, in *Giant Resonances in Atoms, Molecules and Solids*, Vol. 151 of *NATO Advanced Study Institute, Series B: Physics*, edited by J. P. Connerade, J. M. Esteva, and P. C. Karnatak (Plenum, New York, 1987), p. 473; U. Becker, R. Hölzel, H. G. Kerkhoff, B. Langer, D. Szostak, and R. Wehlitz, in *Abstracts of Contributed Papers, 14th International Conference on the Physics of Electronic and Atomic Collisions, Palo Alto, 1985*, edited by M. J. Coggiola, D. J. Huestis, and R. Saxon (ICPEAC, Palo Alto, 1985), p. 12. Both papers present the results of the same measurements, but in the former paper corrected data are given.

[2]U. Becker, H. G. Kerkhoff, M. Kupsch, B. Langer, A. Sivasli, and R. Wehlitz (unpublished). There are more recent experimental data than reported in Ref. 1, which give the 4*d* branching ratio and photoelectron asymmetry parameter in addition to the cross section.

[3]F. Wuilleumier (private communication).

[4]M. Richter, M. Meyer, M. Pahler, T. Prescher, E. V. Raven, B. Sonntag, and H. E. Wetzel (unpublished).

[5]F. Combet-Farnoux, in *Proceedings of the International Conference on Inner Shell Ionization Phenomena and Future Applications, Atlanta, Georgia, 1972,* edited by R. W. Fink, S. T. Manson, J. M. Palms, and R. V. Rao (U.S. Atomic Energy Commision, Oak Ridge, Tennessee, 1973), Vol. 2, p. 1130.

[6]A. W. Fliflet, R. L. Chase, and H. P. Kelly, J. Phys. B **7**, L443 (1974).

[7]G. Wendin, Phys. Lett. **46A**, 119 (1973); in *Vacuum Ultraviolet Radiation Physics,* edited by E. E. Koch, R. Haensel, and C. Kunz (Vieweg-Pergamon, Braunschweig, 1974), p. 225; Phys. Lett. **51A**, 291 (1975); in *New Trends in Atomic Physics,* Proceedings of the Les Houches Summer School of Theoretical Physics, 1982, edited by G. Grynberg and R. Stora (North-Holland, Amsterdam, 1984), p. 555.

[8]M. Ya. Amusia, in *Vacuum Ultraviolet Radiation Physics,* edited by E. E. Koch, R. Haensel, and C. Kunz (Vieweg-Pergamon, Braunschweig, 1974), p. 205.

[9]M. Ya. Amusia, V. K. Ivanov, L. V. Chernysheva, Phys. Lett. **59A**, 191 (1976).

[10]H. P. Kelly, S. L. Carter, B. E. Norum, Phys. Rev. A **25**, 2052 (1982).

[11]A. Zangwill and P. Soven, Phys. Rev. Lett. **45**, 204 (1980); Phys. Rev. A **21**, 1561 (1980); K. Nuroch, M. J. Scott, and E. Zaremba, Phys. Rev. Lett. **49**, 862 (1982).
[12]J. P. Connerade and M. W. D. Mansfield, Proc. R. Soc. London, Ser. A **341**, 267 (1974).
[13]P. Rabe K. Radler, and H. W. Wolf, in *Vacuum Ultraviolet Radiation Physics,* edited by E. E. Koch, R. Haensel, and C. Kunz (Vieweg-Pergamin, Braunschweig, 1974), p. 247.
[14]T. B. Lucatorto, T. J. McIlrath, J. Sugar, and S. M. Younger, Phys. Rev. Lett. **47**, 1124 (1981).
[15]M. M. Hecht and I. Lindau, Phys. Rev. Lett. **47**, 821 (1981).
[16]M. Ya. Amusia and N. A. Cherepkov, Case Stud. At. Phys. **5**, 47 (1975).
[17]W. R. Johnson and C. D. Lin, Phys. Rev. A **20**, 978 (1979); W. R. Johnson, C. D. Lin, K. T. Cheng, and C. M. Lee, Phys. Scr. **21**, 409 (1980).
[18]H. Siegbahn and L. Karlsson, in *Corpuscles and Radiation in Matter I,* Vol. 31 of *Encyclopedia of Physics,* edited by W. Mehlhorn (Springer-Verlag, Berlin, 1982), p. 215.
[19]W. R. Johnson and K. T. Cheng, Phys. Rev. A **20**, 978 (1979).
[20]K. -N. Huang, W. R. Johnson, and K. T. Cheng, At. Data Nucl. Data Tables **26**, 33 (1981).
[21]I. P. Grant *et al.*, Comput. Phys. Commun. **9**, 31 (1980).
[22]M. Kutzner, Z. Altun, and H. P. Kelly (unpublished).
[23]N. A. Cherepkov, Zh. Eksp. Teor. Fiz. **65**, 933 (1973) [Sov. Phys.—JETP **38**, 463 (1974)]; C. M. Lee, Phys. Rev. A **10**, 1598 (1974).
[24]K. -N. Huang, Phys. Rev. A **22**, 223 (1980).
[25]J. W. Cooper, Phys. Rev. Lett. **13**, 762 (1964).
[26]*Giant Resonances in Atoms, Molecules and Solids,* Vol. 151 of *NATO Advanced Study Institute, Series B: Physics,* edited by J. P. Connerade, J. M. Esteva, and P. C. Karnatak (Plenum, New York, 1987).
[27]K. T. Cheng and W. R. Johnson, Phys. Rev. A **28**, 2820 (1983).